

## High Pressure X-ray Diffraction Studies on a Natural Talc

천연산 활석에 대한 고압 X-선 회절연구

Young-Ho Kim (김영호) · Zeon Yi (이지은)

Department of Earth and Environmental Sciences & Basic Science Research Institute,  
Gyeongsang National University, Jinju 660-701, Korea  
(경상대학교 지구환경과학과 및 기초과학연구소)

**ABSTRACT**: Talc ( $Mg_3Si_4O_{10}(OH)_2$ ), one of the sheet silicate minerals, which is the hydrothermal alteration product of serpentinite at Cheongarm mine was prepared for the high pressure compressibility studies. Energy dispersive X-ray diffraction experiment was carried out using the Synchrotron Radiation with the Mao-Bell type diamond anvil cell at room temperature. Polycrystalline talc was mixed with MgO powder for pressure sensor as well as pressure medium in the sample chamber. High pressure runs were performed at pressures up to 35.2 GPa. Talc shows no phase transition within the present high pressure region. Bulk modulus of this talc was determined by the Birch-Murnaghan equation of state to be 78 GPa assuming its first pressure derivative  $K_0'$  of 4.

**요약**: 경상분지 서부에 있는 청암 활석광산에서 채취한 활석은 사문암이 열수변질작용을 받아 생성되어진 층상 규산염광물이다. 이 활석에 대하여 고압하에서 압축성에 대한 연구로 에너지분산 X-선 회절실험을 마오-벨형 다이아몬드 앤빌 기기를 이용하여 상온에서 35.2 GPa까지 시행하였다. 압력 값은 MgO 분말의 상대방정식을 이용하여 측정하였고, 이 분말은 시료방에서 압력의 전달매체로서의 역할도 한다. 활석은 상온에서 현재 시행한 압력하에서 어떠한 상변이도 보이지 않으며, 버치-머내한 상대방정식을 이용하여 체적탄성률을 78 GPa로 결정되었다. 이때 압력에 대한 체적탄성률의 변화율은 4로 가정하였다.

### INTRODUCTION

Talc ( $Mg_3Si_4O_{10}(OH)_2$ ), one of the sheet structured Mg-silicates, is the secondary mineral which is produced by the processes of alteration as well as metasomatism. This mineral has been found in a number of different types of geological environments. It occurs as an alteration product of serpentine (Chidester, 1968) and as a dredge from the ocean floor (Siever

and Kastner, 1967). In Korea, the formation of economically valuable talc deposits is generally restricted to the two geologic environments : metamorphosed siliceous dolomitic carbonate rocks (Lee, 1987; Lee, 1994) and altered ultramafic rock bodies (Lee, 1994; Lee and Choi, 1994; Yun et al., 1994; Kim and Kim, 1997). It is known that high quality talc deposits were originated from dolomite, while the large-quantity of talc deposits was from

serpentinite. Talc deposits originated from both ultramafic rocks and serpentinite of Cheongarm area were made through the alteration involving little chemical transfer since the chemical composition of the primary rocks is relatively similar to talc or talc-serpentine mixtures. On the other hand, synthetic talc can be easily made by the hydrothermal reactions of the starting constituent oxides under high pressure-temperature conditions (i.e., 200 MPa, 600°C) (Cho and Kim, 1997).

Understanding how volatiles are retained and transported in the Earth is important in constraining the processes such as partial melting above subducting plates, metasomatism of mantle and deep crustal minerals, and rheology of the Earth interior (Thompson, 1992). It's been reported that more than five times of water content in the Earth hydrosphere exists at the mantle (Liu, 1986). Possible water reservoirs in the mantle include volatile rich magmas, free fluids and hydrous minerals. In order to get informations about the role that hydrous minerals play in the mantle water stock, more knowledge concerning their properties under the mantle conditions is needed. Hydrous minerals, therefore, have been studied widely in modelling the water budget at the mantle of the Earth. The equation of state (EOS) of various hydrous minerals have been measured under the simulated mantle conditions (Simakov et al., 1974; Finger and Prewitt, 1989; Meade and Jeanloz, 1990; Duffy et al., 1991; Tyburczy et al., 1991; Fei and Mao, 1993; Xu et al., 1994; Mao et al., 1994). Talc, one of the hydrous minerals, could be addressed to access to these situations of the mantle.

In seismology, a number of the mechanisms of earthquake have been proposed so far,

however, none has reached to the complete explanation yet. One of these proposals is the pressure-induced dehydration and amorphization of hydrous mineral phase (Irifune et al, 1996). The amorphization involves the transition of a crystal to a disordered glass-like structure at high pressure. In view of this, phase transitions in the MgO-SiO<sub>2</sub>-H<sub>2</sub>O system have been extensively investigated at high pressures and temperatures (Yamamoto and Akimoto, 1977; Chernosky et al., 1985). Bowen and Tuttle (1949) first studied phase transformations of serpentine and found out that serpentine decomposes into forsterite + talc + water in the temperature range 500~510°C in the entire pressure range investigated. Furthermore, in the pressure range 4.0~7.7 GPa, Yamamoto and Akimoto (1977) discovered other phase assemblages having the serpentine composition. If hydrous silicates can be trapped in the subducting lithosphere at depths greater than 220 km, the effect of H<sub>2</sub>O on the phase transitions displayed in the MgO-SiO<sub>2</sub> system becomes very important to our understanding the phase transitions in the descending lithosphere at great depth (Liu, 1986). Therefore, talc decomposed from serpentine becomes important to assess the situation along the subducting slab.

The research for amorphization of serpentine at high temperature and pressure conditions has been performed (Irifune et al., 1996). These results suggest that amorphization of serpentine is an unlikely mechanism for generating deep-focus earthquakes, as the temperatures of subducting slabs are significantly higher than those of the rapid crystallization regime. Under this regime, it would be worthwhile to investigate the phase transition study on talc to explain these mechanisms as one of the

hydrous minerals.

One purpose of this study is to determine the compressional property of talc at room temperature (i.e., equation of state). The other is to investigate for any phase transformation(s) including amorphization under high pressure at the same temperature condition. One rationale for studying talc, in particular, is that its stability region under pressure and temperature has been investigated widely using various methods, yet no compressibility measurements have been made on the powdered talc samples in the diamond anvil cell at room temperature condition.

## EXPERIMENTAL METHODS

### Sample

Talc ore is traceable along the mafic dike intruded the foliation plane of meta-porphyrritic gneiss at the Cheongarm mine area. Talc ore consists of talc itself together with a small amount of serpentine, olivine and phlogopite. In this experiment, specimens were prepared to be adequate for the chemical analysis and X-ray diffraction (XRD) studies. For the XRD experiment, sample grains were crushed and then ground into fine powder less than 10  $\mu\text{m}$  in diameter using agate mortar. Electron Probe Micro Analysis (CAMECA, SX-51) has been performed on the prepared thin section for analysis of the chemical composition and elemental distribution of talc ore. Analysis conditions were 15 kV/20 mA.

### Experimentals

Angular dispersive X-ray diffraction (ADXRD) method (RIGAKU model D1 Max-3C) was

used for both mineral identification and crystal structure analysis of talc as well as various minerals around ore body. XRD patterns were obtained by Ni-filtered Cu-K $\alpha$  radiation at 40 kV/30 mA in continuous scanning mode at the scanning speed of 10° 2 $\theta$ /min.

*In-situ* high pressure XRD experiments were carried out at the beam port X-17C of the National Synchrotron Light Source (NSLS), Brookhaven National Laboratory using Synchrotron Radiation (SR) and the energy dispersive X-ray diffraction (EDXRD) technique. Polychromatic X-radiation from the superconducting wiggler beam was collimated by two pairs of slits and impinged on the sample. EDXRD patterns of the sample were obtained with an intrinsic-Ge solid state detector (SSD) (Princeton  $\gamma$ -Tech, IGP25-HT). This SSD operates at the liquid nitrogen temperature (77 K) with a bias voltage of 0.3 kV. The diffraction angle was set at  $2\theta = 8^\circ$  (i.e.,  $E \cdot d = 88.426$ ), where  $E$  is the energy of the X-ray photon in keV, and  $d$  is the interplanar spacing in Å. Data were acquired through the multi channel analysis (MCA) system of 4096 channels. Present experiment was gradually carried out with the storage ring operating at 2.5 GeV and 250 to 180 mA. Before the experiment, the relationship between photon energy and channel in MCA was established using variable X-ray sources (Cu, Rb, Mo, Ag, Ba, Tb).

Mao-Bell type DAC was used for the compression of talc. A schematic cross-sectional view of piston-cylinder part of this DAC was given in elsewhere (Kim and Na, 1994). Diamond anvils are of the gem quality. Sample was compacted into the circular hole of gasket between upper (600/300  $\mu\text{m}$ ) and lower diamond anvils (500  $\mu\text{m}$ ). Gasket material used is T301

**Table 1.** Chemistry of talc by EPMA.

	#1	#2	#3	average
SiO <sub>2</sub>	60.23	59.90	59.58	59.01
TiO <sub>2</sub>	0.05	0.02	0.06	0.04
Al <sub>2</sub> O <sub>3</sub>	0.66	1.23	2.00	1.30
FeO*	0.38	0.46	0.33	0.39
MnO	0.00	0.00	0.07	0.02
MgO	33.68	32.98	32.13	32.93
CaO	0.03	0.02	0.00	0.02
Na <sub>2</sub> O	0.04	0.06	0.09	0.06
K <sub>2</sub> O	0.02	0.08	0.71	0.27
Total	95.105	94.762	94.968	94.945
Number of cations on the basis of 22 oxygens				
Si	7.689	7.647	7.606	7.647
Al	0.099	0.186	0.301	0.195
Tot. tet.**	7.788	7.833	7.907	7.843
Fe	0.041	0.050	0.035	0.042
Mn	0	0	0.007	0
Mg	6.410	6.277	6.115	6.267
Na	0.010	0.014	0.021	0.015
K	0.004	0.014	0.115	0.044
Tot. oct.**	6.455	6.355	6.293	6.368

\* All ions reported FeO.

\*\* Total number of cations in tetrahedral and octahedral site.

stainless steel alloy metal plate, and hole dimension is 150  $\mu\text{m}$  in diameter. Pressure was applied on the gasketed powder sample by driving the lower anvil against the stationary upper anvil by rotating a driving screw with wrench.

## RESULTS AND DISCUSSIONS

Chemistry of this natural talc determined by EPMA is given in Table 1. Chemical formula of talc has been calculated to be  $(\text{Mg}_{6.267}\text{Fe}_{0.042})(\text{Si}_{7.647}\text{Al}_{0.195})\text{O}_{20}(\text{OH})_4$ . Talc, usually,

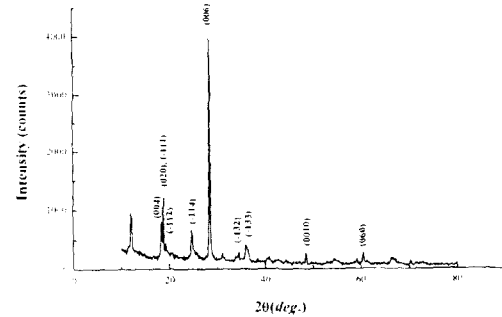


**Fig. 1.** Spectrum by ADXR D method on talc at 1 bar.

shows a little variations in chemical composition from the end-member formula of  $\text{Mg}_3[\text{Si}_4\text{O}_{10}](\text{OH})_2$ , being substituted commonly up to about 0.15 Al replacing Si and about 0.1 Fe replacing Mg (Deer et al., 1962).  $\text{H}_2\text{O}$  contents are close to 4.7 wt% normally. Comparing the chemical composition with an ideal chemistry of talc, the content of Mg is higher than that of the ideal formula. Other elements such as Mn, Na and K also may substitute magnesium, but are more likely to be present as interlayer ions or in impurities.

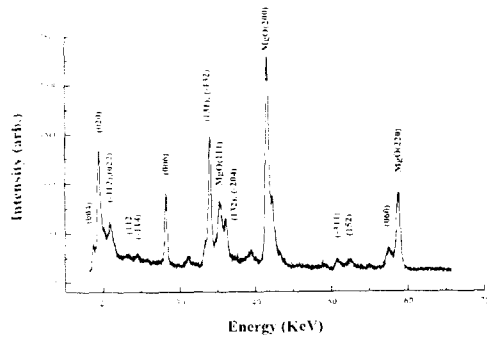
Under normal conditions, talc crystallizes in the monoclinic structure, with space group  $\text{C2/c}(15)$ . Starting phase of talc identified using the ADXR D method at 1 bar (i.e., 0.0001 GPa) were indexed to an monoclinic crystal system using JCPDS XRD data file (talc (19-770)) (Fig. 1 and Table 2). EDXR D patterns of the same sample is shown in Fig. 2 and listed in Table 3, respectively. Although the sample used is same in both experiments, there are somewhat differences between ADXR D and EDXR D patterns. The most remarkable difference is the intensity of (006) peak. But, positions of peaks are in coincidence with each other. The difference between two XRD patterns would be due to absorption of the

**Table 2.** ADXRD data of talc at ambient conditions.

$I/I_0^*$	$d_{\text{obs}}(\text{\AA})$	$d_{\text{cal}}(\text{\AA})$	(hkl)
20	4.700	4.695(7)	(004)
30	4.599	4.588(0)	(020), (-111)
10	4.374	4.340(4)	(-112)
5	4.211	4.122(2)	(022)
25	3.601	3.541(1)	(-114)
100	3.130	3.130(8)	(006)
10	2.600	2.599(0)	(-132)
25	2.495	2.511(0)	(-133)
10	1.877	1.878(9)	(0010)
10	1.530	1.529(3)	(060)

\* Relative intensities, visually determined.

Lattice parameters were calculated on the basis of the present experimental data;  $a = 5.275(4)$   $\text{\AA}$ ,  $b = 9.176(1)$   $\text{\AA}$ ,  $c = 19.127(6)$   $\text{\AA}$ ,  $\beta(\text{deg.}) = 100.99(7)$ ,  $V_m = 908.91(3)$   $\text{cm}^3/\text{mol}$ .


**Fig. 2.** Spectrum by EDXRD method on talc in the diamond anvil cell at 1 bar.

radiations at both the diamond windows themselves and the intrinsic Ge-window of the SSD, and the limitation of the  $2\theta$  range in the EDXRD technique configuration. Furthermore, (002) peak is not shown in both XRD patterns, which is the most strong XRD peak of talc.

The diagnostic reflection peaks of talc are 4.599  $\text{\AA}$  (020, -111), 3.601  $\text{\AA}$  (-114), 3.130

**Table 3.** EDXRD data of talc at ambient conditions.

$I/I_0^*$	$d_{\text{obs}}(\text{\AA})$	$d_{\text{cal}}(\text{\AA})$	(hkl)
10	4.752	4.67(0)	(004)
100	4.558	4.58(5)	(020)
40	4.231	4.11(8)	(-112), (022)
15	3.780	3.83(5)	(112)
15	3.416	3.55(6)	(-114)
70	3.122	3.11(3)	(006)
90	2.607	2.57(9)	(131), (-132)
40	2.438	2.47(0)	(-204), (132)
30	2.232	2.24(1)	(-223)
10	2.077	2.08(3)	(135)
20	1.727	1.74(9)	(-311)
20	1.671	1.70(7)	(152)
20	1.529	1.54(2)	(060)

\* Relative intensities, visually determined.

Lattice parameters were calculated based on the present experimental data;  $a = 5.286(8)$   $\text{\AA}$ ,  $b = 9.128(3)$   $\text{\AA}$ ,  $c = 18.942(4)$   $\text{\AA}$ ,  $\beta(\text{deg.}) = 99.18(9)$ ,  $V_m = 902.28(3)$   $\text{cm}^3/\text{mol}$ .

$\text{\AA}$  (006), 2.600  $\text{\AA}$  (-132), 2.495  $\text{\AA}$  (-133), 1.877  $\text{\AA}$  (0010), and 1.530  $\text{\AA}$  (060) (Table 2). Unit cell contains  $Z = 4$  per formula. Lattice parameters of talc by ADXRD are as follows;  $a = 5.275(4)$   $\text{\AA}$ ,  $b = 9.176(1)$   $\text{\AA}$ ,  $c = 19.127(6)$   $\text{\AA}$ ,  $\beta(\text{deg.}) = 100.99(7)$ , and  $V_m = 908.91(3)$   $\text{cm}^3/\text{mol}$ . On the other hand, those by EDXRD are as follows;  $a = 5.286(8)$   $\text{\AA}$ ,  $b = 9.128(3)$   $\text{\AA}$ ,  $c = 18.942(4)$   $\text{\AA}$ ,  $\beta(\text{deg.}) = 99.18(9)$ ,  $V_m = 902.28(3)$   $\text{cm}^3/\text{mol}$ . Compared with two volume data, EDXRD one is slightly smaller than that of ADXRD. This kind of difference is common in high pressure compression experiment because it is hardly to set the sample pressure in the diamond anvil cell to the ambient pressure condition manually. Even if there exist this kind of drawback in the DAC experiment, EDXRD value at 0.0001 GPa (i.e.,

**Table 4.** Lattice parameters of talc with pressure.

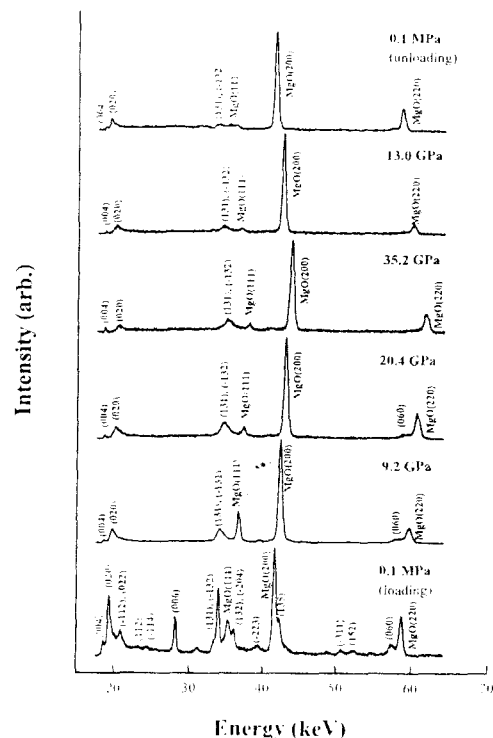
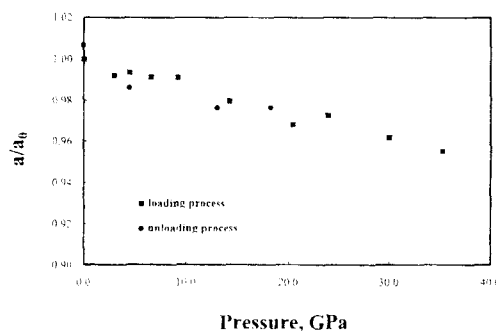
P, GPa	a, Å	b, Å	c, Å	$\beta$ , deg	$V_m$ , cm <sup>3</sup> /mol
0.0001	5.286	9.128	18.942	99.18	903.283
3.0	5.244	9.044	18.462	100.00	862.278
4.5	5.252	9.074	17.785	97.42	840.477
6.6	5.240	9.071	17.852	98.60	839.003
9.2	5.239	9.048	17.852	98.61	836.662
14.2	5.179	8.962	16.653	100.96	758.789
20.4	5.118	8.919	16.110	98.51	727.218
23.9	5.141	8.894	16.032	99.58	722.793
30.0	5.084	8.797	16.160	99.40	713.136
35.2	5.050	8.758	16.347	100.76	710.316
28.0*	5.258	8.779	16.084	100.21	730.674
18.2*	5.162	8.907	16.783	102.05	754.664
13.0*	5.162	8.928	17.463	101.91	787.565
4.5*	5.213	9.051	17.720	100.82	821.287
0.0001*	5.322	9.162	19.362	94.17	941.556

\* unloading process.

1 bar) was selected for the further analysis of the compressibility of talc.

In total, 15 high pressure runs were performed at pressures up to 35.2 GPa. Pressure of the sample was gradually increased to 35.2 GPa. Sample consists of a mixture of powdered talc and MgO, which serves as an internal pressure standard and pressure medium. XRD pattern, therefore, consists of the diffraction peaks both from talc itself and MgO. Peaks of (111), (200) and (220) of MgO were employed for the pressure determinations using its well known equation of state (Manghnani et al., 1984).

With increasing pressures, XRD peaks of (004), (020), (131), (-132), (060) maintain considerable intensities, thus, these XRD peaks were used for determinations of the unit cell parameters at each high pressure. Table 4

**Fig. 3.** A series of energy dispersive spectra of talc with pressure both loading and unloading processes at room temperature.**Fig. 4.** Compressibility of a-axis of talc.

summarizes the results from the present high pressure work. At the same time, a series of spectra selected at the appropriate interval are shown in Fig. 3. This figure shows the change of lattice-plane spacings with both loading and

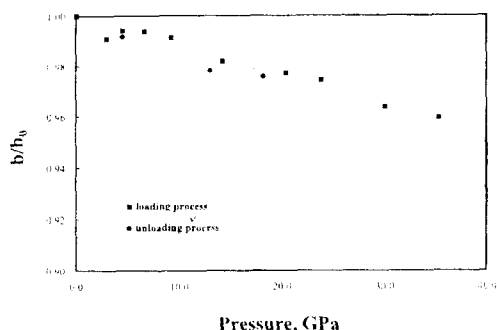


Fig. 5. Compressibility of b-axis of talc.

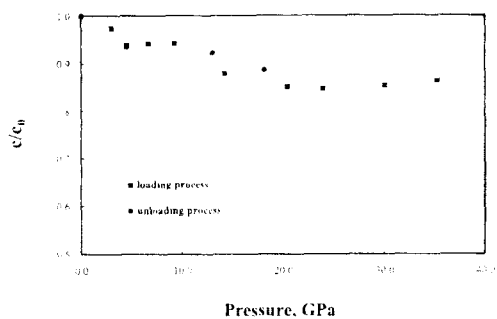


Fig. 6. Compressibility of c-axis of talc.

unloading processes. EDXRD spectra show no phase transition with pressures. Compression data,  $a/a_0$ ,  $b/b_0$ ,  $c/c_0$  and  $V/V_0$  are plotted in Figs. 4, 5, 6 and 7, respectively. These figures show variations the pressure dependence of the relative lattice parameters and volume changes, respectively. As can be seen in these figures, all of these values decrease on loading process from 0.0001 GPa to 35.2 GPa, however, increase at each pressure on unloading process from 35.2 GPa to 0.0001 GPa. The volume was calculated from the refined unit-cell parameters at each high pressure. The pressure-volume data obtained in this way (Table 4 and Fig. 7) have been subsequently fitted to the Birch-Murnaghan equation of state :

$$P = 1.5K_0[X^{(7/3)} - X^{(5/3)}][1 - \xi(X^{(2/3)} - 1)]$$

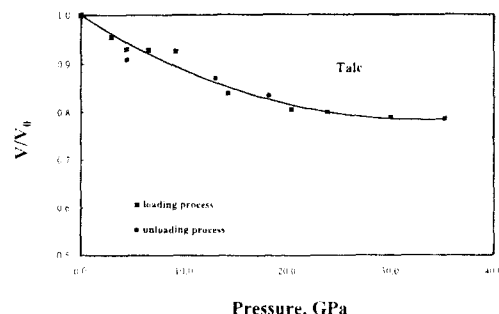


Fig. 7. Volume compressibility of talc.

**Table 5.** Zero pressure bulk modulus ( $K_0$  in GPa) in the sheet structured silicate minerals and related compounds.

compounds	$K_0$	reference
$\text{KMg}_3\text{AlSi}_3\text{O}_{10}(\text{F},\text{OH})_2$ (Phlogopite)	$58.5 \pm 2$	Hazen and Finger (1978)
$(\text{Mg},\text{Fe},\text{Al})_6(\text{Si},\text{Al})_4\text{O}_{10}$ ( $\text{F},\text{OH})_2$ (Chlorite)	$55.0 \pm 10$	Hazen and Finger (1978)
$\text{KAl}_3\text{Si}_3\text{O}_{10}(\text{OH})_2$ (Muscovite)	$61.4 \pm 4$	Faust and Knittle (1993)
$\text{BaFeSi}_4\text{O}_{10}$ (Gillepsite I)*	$62 \pm 3$	Hazen and Finger (1983)
$\text{BaFeSi}_4\text{O}_{10}$ (Gillepsite II)**	$66 \pm 3$	Hazen and Finger (1983)
$\text{Mg}_3\text{Si}_4\text{O}_{10}(\text{OH})_2$ (Talc)	$78 \pm 3$	This study

\* low-pressure tetragonal structure.

\*\* high-pressure orthorhombic structure.

where  $X = V_0/V$ ,  $\xi = 3/4(K_0' - 4)$  and  $K_0' = (dK/dP)_T$ ,  $V_0$ , volume at zero pressure and  $V$ , volume at pressure  $P$ . Here,  $K_0$  and  $K_0'$  are the isothermal bulk modulus and its first pressure derivative, respectively evaluated at zero pressure (i.e., 1 bar). The parameters  $K_0$  and  $K_0'$  are refined by a least-square method. Based on the present data and the Birch-Murnaghan equation of state, bulk modulus was determined to be  $78 \pm 3$  GPa assuming its  $K_0'$  of 4. Table 5 shows

the bulk moduli of the several layered silicate minerals and the structural analogs to talc at zero pressure. The bulk modulus of talc is larger than those of most sheet silicate minerals which have relatively small bulk moduli such as phlogopite, chlorite, and muscovite. Because this natural talc contains impurities as shown in Table 1, bulk modulus appears a little too high. The present experiment, furthermore, was performed in the non-hydrostatic conditions. This might be contributed a further effect: a slightly higher bulk modulus of talc than a possible measured value under hydrostatic condition.

Most hydroxides crystallize in a layered structure. In this structure, hydrogen bonds connect, and the compression mainly takes place in such layers and it causes the small bulk modulus. If the impurities of talc exist between layers, these might cause to resist against the compression along layers and appear to increase the bulk modulus of the present natural talc. The structure of chlorite is one of the regularly alternating talc-like and brucite-like sheets. The bulk modulus of brucite itself is known to be 54.3 GPa (Fei and Mao, 1993). When we take the average of the bulk modulus of brucite and talc, chlorite value of  $55 \pm 10$  GPa by Hazen and Finger (1978) would be acceptable within the standard deviation.

At present result, it cannot be ruled out phase transition from monoclinic system to orthorhombic system. It is difficult, however, to identify the  $\beta$  variations due to the limitation of EDXRD analysis. From this point of view, it is recommended that the high pressure Rietveld refinement in the future ADXRD results using the imaging plate experiment in conjunction with Synchrotron Radiation.

There is a good possibility that hydrous magnesian silicates exist in the subducting lithosphere according to Liu (1986) if the hydrous phases, such as talc, can be preserved as well as decomposed from serpentine in the subducting lithosphere. It is hardly to address the problem related to the earthquake mechanism based on the present experiment result which was done at room temperature condition. However, talc, if it be delivered or existed, may affect on the occurrence of intermediate or deep focus earthquake in the mantle by dehydration as well as any possible phase transformation(s). More data extended to the high temperature with high pressure region are needed to access this kind of the Earth interior phenomenon. Present experiment result, however, satisfies the rationale for studying the talc because this is the first approach to measure the compressibility of the powdered talc in the diamond anvil cell at room temperature condition.

## CONCLUSIONS

Polycrystalline talc from Cheongarm mine was compressed for the equation of state studies at room temperature conditions. High pressure experiment has been carried out at the X17C beam port of the NSLS using Mao-Bell type diamond anvil cell and Synchrotron Radiation with the energy dispersive X-ray diffraction technique. The present experimental results are as follows : Talc compressed up to 35.2 GPa shows no phase transition at room temperature. Bulk modulus of talc was determined to be  $78 \pm 3$  GPa with  $K_0'$  of 4.0 (assumed value) by fitting to the Birch-Murnaghan equation of state. This result shows the bulk modulus of talc is larger than those of the sheet silicates minerals such as



phlogopite, muscovite, and chlorite.

## ACKNOWLEDGMENTS

Authors appreciate Prof. L. C. Ming for his cooperations for the high pressure X-ray diffraction experiments at the X-17C of the National Synchrotron Light Source, Brookhaven National Laboratory, U.S.A. He is at the Mineral Physics Group, Hawaii Institute of Geophysics and Planetology, School of Ocean and Earth Sciences and Technology, The University of Hawaii at Manoa. EPMA has been performed with aid of Mr. Lee, S. H. at the KBSI, Daejon. This study was supported by the Basic Science Research Institute Program (BSRI 97-5402, Ministry of Education & 1998-015-D00263, Korea Research Foundation).

## REFERENCES

- Bowen, N. L. and Tuttle, O. F. (1949) The system MgO-SiO<sub>2</sub>-H<sub>2</sub>O. *Bull. Geol. Soc. Am.*, 60, 117-120.
- Chernosky, J. V., Day, H. W. and Caruso, L. J. (1985) Equilibria in the system MgO-SiO<sub>2</sub>-H<sub>2</sub>O: experimental determination of the stability of Mg-anthophyllite. *Am. Mineral.*, 70, 223-236.
- Chidester, A. H. (1968) Evolution of the ultramafic complexes of northwestern New England, In : E-an Zen, White, W. S., Hadley, J. B. and Thompson, J. B. (Eds.) *Study of the Appalachian Geology Northern Maritime*. Interscience, John Wiley & Sons, NY, 343-354.
- Cho, D. S. and Kim, H. S. (1993) The high temperature stability limit of talc, Mg<sub>3</sub>Si<sub>3</sub>O<sub>10</sub>(OH)<sub>2</sub>. *J. Petrol. Soc. Korea*, 6(2), 123-132.
- Deer, W. A., Howie, R. A. and Zussman, J. (1962) *Rock-forming minerals*, v3: Sheet silicates. Longman, London, 270.
- Duffy, T. S., Ahrens, T. J. and Lange, M. A. (1991) Shock wave equation of state of brucite Mg(OH)<sub>2</sub>. *J. Geophys. Res.*, 9, 14319-14330.
- Faust, J. and Knittle, E. (1993) The equation of state, amorphization and high-pressure phase diagram of muscovite. *J. Geophys. Res.*, 99(B10), 19785-19792.
- Fei, Y. and Mao, H. K. (1993) Static compression of Mg(OH)<sub>2</sub> to 78 GPa at high temperature and constraints on the equation of state of fluid H<sub>2</sub>O. *J. Geophys. Res.*, 98, 11875-11884.
- Finger, L. W. and Prewitt, C. T. (1989) Predicted composition for high-density hydrous magnesium silicates. *Geophys. Res. Lett.*, 16, 1395-1397.
- Hazen, R. M. and Finger, L. W. (1978) The crystal structures and compressibilities of layer minerals at high pressures. II. phlogopite and chlorite. *Am. Mineral.*, 63, 293-296.
- Hazen, R. M. and Finger, L. W. (1983) High pressure and high temperature crystallographic study of the gillepsite I-II phase transition. *Am. Mineral.*, 68, 595-603.
- Irifune, T., Kuroda, K., Funamori, N., Uchida, T., Yagi, T., Inoue, T. and Miyajima, N. (1996) Amorphization of serpentine at high pressure and high temperature. *Science*, 272, 1468-1469.
- Kim, G. Y. and Kim, S. J. (1997) Chemistry of talc ores in relation to the mineral assemblages in the Yesan-Gonju-Cheongyang area, Korea. *J. Miner. Soc. Korea*, 10, 60-73.
- Kim, Y. H. and Na, K. C. (1994) High pres-

- sure X-ray diffraction study on a graphite using Synchrotron Radiation. *J. Petrol. Soc. Korea*, 3(1), 34-40.
- Lee, C. H. (1987) Origin of talc deposit in the Chungju area: Origin and types of initial rocks and their origin. *J. Geol. Soc. Korea*, 23(2), 173-188.
- Lee, S. H. (1994) Phase equilibria between coexisting minerals in the talc ores and process of talc formation in the Daeheung Talc Deposits, Korea. *J. Petrol. Soc. Korea*, 3(2), 156-170.
- Lee, S. H. and Choi, G. J. (1994) Geochemistry and chemical equilibria of coexisting minerals in the gneisses around the Daeheung Talc Deposits, Korea. *J. Petrol. Soc. Korea*, 3(2), 138-155.
- Liu, L. G. (1986) Phase transformations in serpentine at high pressures and temperatures and implications for subducting lithosphere. *Phys. Earth Planet. Inter.*, 42, 255-262.
- Manghnani, M. H., Ming, L. C., Balogh, J., Skelton, E. F., Qadri, S. B. and Schiferl, D. (1984) Use of the internal pressure calibrants *in-situ* in X-ray diffraction measurements at high pressure and temperature: Review and recent results. *High Temperature-High Pressures*, 16, 563-571.
- Mao, H., Shu, J., Hu, J. and Hemley, R. J. (1994) High-pressure X-ray diffraction study of diaspore. *S. S. Communications*, 90, 497-500.
- Meade, C. and Jeanloz, R. (1990) Static compression of  $\text{Ca}(\text{OH})_2$  at room temperature: Observations of amorphization and equation of state measurements to 10.7 GPa. *Geophys. Res. Lett.*, 17, 1157-1160.
- Siever, R. A. and Kanster, M. (1967) Mineralogy and petrology of some Mid-Atlantic Ridge Sediments. *J. Marine Res.*, 25, 263-278.
- Simakov, G. V., Pavlovskiy, M. N., Kalashnikov, N. G. and Trunin, R. F. (1974) Shock compression of twelve minerals. *Izvestiya Earth Phys.*, 10, 11-17.
- Thompson, A. B. (1992) Water in the Earth's upper mantle. *Nature*, 358, 295-302.
- Tyburczy, J. A., Duffy, T. S., Ahrens, T. J. and Lange, M. A. (1991) Shock wave equation of state of serpentine to 150 GPa: implications for the occurrence of water in the Earth's lower mantle. *J. Geophys. Res.*, 96, 18011- 18027.
- Yamamoto, K. and Akimoto, S. (1977) The  $\text{MgO-SiO}_2\text{-H}_2\text{O}$  at high pressures and temperature stability field for hydroxyl-chondrodite, hydrosyl-clino and 10 Å-phase. *Am. J. Sci.*, 277, 288-312.
- Xu, J. A., Hu, J., Ming, L. C., Huang, E. and Xie, H. (1994) The compression of diaspore,  $\text{AlO}(\text{OH})$  at room temperature. *Geophys. Res. Lett.*, 21, 161-164.
- Yun, S. P., Moon, H. S. and Song, Y. (1994) Mineralogy and genesis of the Pyoungan and Daeheung talc deposits in ultramafic rocks, the Yoogoo area. *Econ. Environ. Geol.*, 27(2), 131-145.